END
DATE
FILMED
10 83
DTIC

1.0 4.5 5.0 5.6 6.3 2.8 2.5
3.2 2.2
3.6
4.0 2.0
1.1
1.8
1.25 1.4 1.6
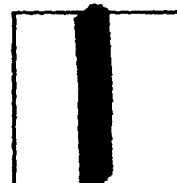
MICROCOPY RESOLUTION TEST CHART
NATIONAL BUREAU OF STANDARDS-1963-A

AD A131956

DTIC ACCESSION NUMBER

LEVEL

II

INVENTORY

Rpt. No. NBDL-80R009

DOCUMENT IDENTIFICATION

Becker, Edward B.;

Aug. '80

DISTRIBUTION STATEMENT A

Approved for public release;
Distribution Unlimited

DISTRIBUTION STATEMENT

ACCESSION FOR		
NTIS GRA&I	☒	
DTIC TAB	☐	
UNANNOUNCED	☐	
JUSTIFICATION		
BY		
DISTRIBUTION /		
AVAILABILITY CODES		
DIST	AVAIL AND/OR SPECIAL	
A		

DISTRIBUTION STAMP

DTIC
S ELECTE
AUG 30 1983
D
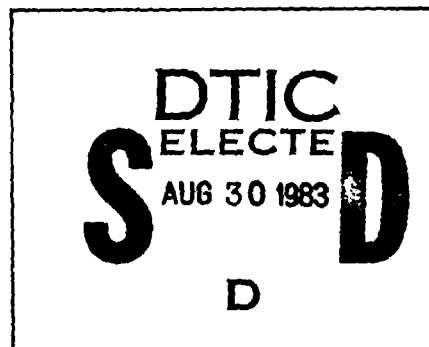
DATE ACCESSIONED

83 08 30 009

DATE RECEIVED IN DTIC

DTIC FORM 70A
OCT 79

DOCUMENT PROCESSING SHEET

NBDL-80R009

HEAD AND NECK KINEMATICS FOR FRONTAL, OBLIQUE, AND LATERAL CRASH IMPACT

Edward B. Becker
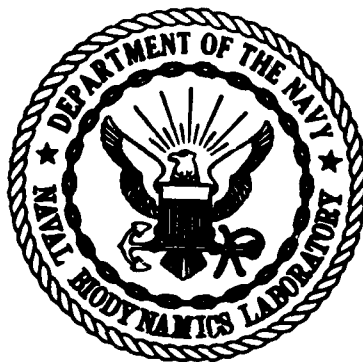
August 1980

NAVAL BIODYNAMICS LABORATORY
New Orleans, Louisiana

SECURITY CLASSIFICATION OF THIS PAGE (When Data Entered)

REPORT DOCUMENTATION PAGE		READ INSTRUCTIONS BEFORE COMPLETING FORM
1. REPORT NUMBER NBDL-80R009	2. GOVT ACCESSION NO.	3. RECIPIENT'S CATALOG NUMBER
4. TITLE (and Subtitle) Head and Neck Kinematics for Frontal, Oblique, and Lateral Crash Impact		5. TYPE OF REPORT & PERIOD COVERED Research Report
		6. PERFORMING ORG. REPORT NUMBER NBDL-80R009
7. AUTHOR(s) Edward B. Becker		8. CONTRACT OR GRANT NUMBER(s) Mod. #1 Interagency Agreement, DOT-HS-7-016471A
9. PERFORMING ORGANIZATION NAME AND ADDRESS Naval Biodynamics Laboratory P.O. Box 29407 New Orleans, LA 70189		10. PROGRAM ELEMENT, PROJECT, TASK AREA & WORK UNIT NUMBERS
11. CONTROLLING OFFICE NAME AND ADDRESS Naval Medical REsearch and Development Command Bethesda, MD 20014		12. REPORT DATE August 1980
		13. NUMBER OF PAGES 46
14. MONITORING AGENCY NAME & ADDRESS(if different from Controlling Office) Department of Transportation, National Highway Traffic Safety Administration, Office of Contracts and Procurement, NAD-30 Washington, D. C. 20590		15. SECURITY CLASS. (of this report) Unclassified
		15a. DECLASSIFICATION/DOWNGRADING SCHEDULE

16. DISTRIBUTION STATEMENT (of this Report)

Approved for public release; distribution unlimited

17. DISTRIBUTION STATEMENT (of the abstract entered in Block 20, if different from Report)

18. SUPPLEMENTARY NOTES

19. KEY WORDS (Continue on reverse side if necessary and identify by block number)

Impact, acceleration, motion, head, neck, musculoskeletal system, kinematics, anthropemetry, anatomical models, mathematical models

20. ABSTRACT (Continue on reverse side if necessary and identify by block number)

High speed photographic coverage of the head and neck of a living human volunteer both for voluntary motion and for oblique and lateral impact was reduced and analysed.

This analysis identifies a range of four-pivot mechanical linkages that can simulate the head and neck kinematics of this volunteer in response to frontal, as well as lateral and oblique impact.

The kinematics of a linkage selected from this range is compared to the kinematics observed in the photography to evaluate the faith with which

DD FORM 1473 EDITION OF 1 NOV 65 IS OBSOLETE
1 JAN 73
S/N 0102-LF-014-6601

it reproduces the filmed data and the similarity to the calculated kinematic trajectories of the volunteer.

ABSTRACT

High speed photographic coverage of the head and neck articulation of a living human volunteer both for voluntary motion and for oblique and lateral impact was reduced and analysed.

This analysis identifies a range of four-pivot mechanical linkages that can simulate the head and neck kinematics of this volunteer in response to frontal, as well as lateral and oblique impact.

The kinematics of a linkage selected from this range is compared to the kinematics observed in the photography to evaluate the faith with which it reproduces the filmed data and the similiarity to the calculated kinematic trajectories of the volunteer.

SYMBOL TABLE

E –   Linearized approximation of the mean square residual error

E_o –   Mean square residual error for a particular geometry

D –   Diagonalized matrix of the second derivatives of E with respect

to variations in the linkage geometry

X' –   Variations in the linkage geometry according to the coordinates of D

T_1 –   Position of the pivot fixed relative to the first thoracic vertebral body

H –   Position of the pivot fixed in the head

L –   Lengths in the linkage

INTRODUCTION

The Naval Aerospace Medical Research Laboratory, New Orleans, Louisiana, is currently engaged in a series of experiments to determine human dynamic response to impact acceleration. In the course of these experiments, human volunteers undergo short duration accelerations approximating frontal, lateral, and oblique crash impact. The resulting motion of the volunteers' heads and first thoracic vertebral bodies is monitored by anatomically mounted clusters of inertial transducers and photographic targets. It is hoped that the study of these motions will contribute to the design of safe and effective impact protection systems for use in all kinds of vehicles.

Perhaps the most useful result of such study will be the development of improved anthropomorphic dummies for use in testing at potentially injurious levels of impact. Differences observed between the impact response of the human volunteers and that of some currently available anthropomorphic dummies show that the dummy neck systems are particularly deficient. (1,2) The subject of this presentation is the first part of a two part approach to developing a dummy neck system suitable for frontal, lateral, and oblique crash impact testing.

This approach is developed from an earlier attempt to identify a dummy neck system suitable for frontal crash impact testing. (3) The first part of the approach is a purely kinematic analysis. All the data for each particular human volunteer is examined to identify a spatial linkage that will reproduce all the head versus first thoracic vertebral body positions observed in the experiments.

There are three aspects to this linkage, its form, its geometry, and its articulation. The form will apply to the whole range of humanity and perhaps even to the primates used in impact testing. The geometry consists of those parameters which apply the general

form to a single individual. These geometrical parameters will vary between individuals but will be constant over each particular individual's entire history barring changes due to injury, disease, or advancing age. The articulation consists of those parameters that identify a particular head versus T-1 position. These articulational parameters vary continuously with time and will become the variables by which an individual's head versus T-1 response to impact will be described.

The second part of this approach will build on the results of the first part. Dynamic elements will be incorporated into the kinematic linkages identified for the various human volunteers so that the entire assembly will simulate the dynamics of the observed impact response as well as the kinematics.

These dynamic elements will consist of springs, dashpots, and frictions that will operate across the linkage articulations. These too, will each have a general form that will serve across the range of experimental subjects but with precise parameters defined for each individual subject.

The success of the approach depends largely on the choice of the linkage form. A poorly chosen form would probably fail in the kinematic analysis, but it is quite possible that a candidate form could satisfy the kinematics and still make impossible demands of the dynamic elements later on. Since the choice of linkage form may be subject to reconsideration and this kinematic analysis exercised a number of times for each form, this presentation will attempt a complete treatment of the kinematic analysis and leave the dynamic analysis to the future.

OVERVIEW

Since the kinematic analysis is largely a study of the relative positions of the head and the first thoracic vertebral body; the primary data used in this analysis is photographic.

2

The photographic system used to acquire this data is essentially that described in ref. 4 although a number of improvements have since been incorporated.

This system acquires high speed films of targets fixed relative to the volunteer's head and first thoracic vertebral body during an impact experiment. The positions of the head and first thoracic vertebral body are calculated by finding those positions for which the theoretical positions of the target images in the film frames most closely resembles the positions actually observed. Given a kinematic linkage of known geometry, the articulational parameters of this linkage are found in exactly the same manner.

Such a kinematic linkage was selected at the outset of this project. This linkage is essentially the two dimensional linkage of ref. 3 with two additional hinges or pivots as shown in figure 1 and described in appendix B.

This four pivot linkage has, within the limits imposed by midsagittal symmetry, nine geometrical parameters. Since the angle formed by the axes of the two interior pivots has been fixed at ninety degrees, only the eight lengths indicated in the figure must be identified.

The identification process is iterative. A likely set of geometrical parameters is selected and compared to the data of a single volunteer. The articulational parameters are fitted for each photographically acquired position of the volunteer and the quality of these fits is examined over the entire data set. This examination suggests a new set of geometrical parameters which are then subjected to the same comparison. Presumably, this process will lead to the best set of geometrical parameters that the linkage form will afford for the particular volunteer.

If this final linkage fits the observed data well, the analysis will be extended to other volunteers or even to the dynamic part of the approach; otherwise, care has been taken to simplify directing the analysis to other forms of linkage.

3

The Photographic Data

In the impact experiments the volunteer wears two clusters of photographic targets, the first fixed as rigidly as possible with respect to the first thoracic vertebral body, the second fixed similarly with respect to the head as shown in figure 2. During impact three sled mounted cameras acquire film images of these targets at nominal rates of 500 frames per second.

After the impact the film from the three cameras is developed and digitized. In this digitization each frame of film is examined to determine the precise time at which it was exposed and the position of each of the target images within the filmplane.

The various processes by which the film images are related to the sled referenced positions of the head and T-1 have been analyzed and quantified. The location of each target in its cluster is measured using a site developed stereovideographic process. The location of the clusters with respect to the anatomical bodies is measured similarly using the stereoradiographic process reported in ref. 5. Optical survey techniques locate each camera within the sled reference system. Finally, the mechanisms by which the cameras produce images are quantified with the camera calibration technique recorded in ref. 4.

It is now a matter of arithmetic to set up algorithms yielding ideal target image positions as functions of the anatomical body positions. These algorithms may then be linearized and used in an iterative process to find the anatomical positions that provide the best fit of the ideal image positions to those observed in the digitization.

These anatomical positions can be solved for all the photographic data yielding time histories of the motion of T-1 and the head in the sled reference system in response to crash impacts. However, there are drawbacks to this direction solution. The nature of the data collection imposes errors that will affect this solution in various ways.

The most serious of these errors are the small biases present in the camera surveys and

4

calibrations. These biases introduce a finite residual difference between the observed image positions and the best fit of the idealized image positions. Although these biases are themselves invariant, the resulting finite residual can impose discontinuous shifts in the calculated trajectories of the head and T-1.

These shifts occur because the motion induced by the impact is generally so large that various targets pass in and out of the camera fields of view during the ɔɑct response. The clusters are arranged so that sufficient targets are visible at any instan· ᵼowever the set of visible targets changes throughcut; and, every time the target set ch ᵼ the presence of an irreducible residual will cause a shift in the trajectory determined by least squares fit.

This phenomenon can be visualized by invoking the mechanical representation of a least squares fit as a series of springs connecting each observation to its ideal counterpart. The best solution is generally that for which the springs are in equilibrium. If a spring is added to or taken from the representation, then the system is no longer in equilibrium and must seek some new equilibrium state. The only exceptions are those cases in which there is perfect agreement between the observation and the ideal counterpart to be added to or dropped from the solution.

While these difficulties can certainly be cured by refining the various input data to eliminate the small biases that are the source of the problem, the algorithms themselves can also be improved. The solution described earlier treats the motion as a collection of isolated positions. By recognizing that the motion is instead a sequence of positions, a ᵼore refined algorithm can control the transitions between equilibrium states imposed by ᵼanging target sets.

This new algorithm shown in ᶠigure 3 can be said to replace the springs of a least squares solution with parallel spring dampers. If an observation is dropped from the solution,

5

the dampers will impose a smooth transition to the new equilibrium. If an observation is added to the solution, the corresponding spring-damper is set to the current equilibrium.

This algorithm uses the straightforward least squares fit to generate a series of small adjustments for each of the photographic image positions. These adjustments are weighted sums of the residual differences between ideal and observed image positions for prior frames of data. These adjustments are then added to the observed image positions to produce a new data set whose solution has no irreducible residual.

This new data set, christened 'arless' data, is then itself subjected to the standard least squares algorithm. Since the residual differences between the ideal and arless image positions are almost nonexistent, changes in the target set produce no shifts in the solution. Furthermore, the solution obtained from this arless data is asymptotic to that of the unadjusted or raw data approaching it at a rate fixed by the weighing scheme used to generate the adjustments.

The Linkage Analysis

Ideally, the kinematic analysis is an attempt to infer the nature of the constraints that the cervical spine imposes on the relative positions of the head and T-1. To be sure, more worldly concerns have also been imposed, these being that the constraints be mobilized as some simple mechanism and further that this mechanism serve in conjunction with simple dynamic elements to reproduce dynamic as well as kinematic response; yet, the kinematic analysis is still the study of constraints.

Since the solution for head and T-1 position obtained by the photographic data system assumes no constraints acting between the head and T-1, no constrained solution can obtain better fit to the observations. Therefore, the photographic solution becomes the baseline for the study, and the arless data obtained by this solution will be the data to which the linkages will be fitted.

6

The form of a likely linkage candidate is shown in figure 1 and described in appendix B. This is a four pivot linkage reducing the head - T-1 system from 12 degrees of freedom, six each for the two anatomical sites; to 10 degrees of freedom, six for say T-1 and four more to obtain the head position.

The solution for these 10 parameters, the six components of the T-1 position plus the four linkage articulations proceeds in exactly the same manner as the standard least squares solution for the head and T-1 positions except that instead of solving for two independent sets of six variables, the solution obtains a single set of 10.

This solution for the 10 parameters will also yield an irreducible residual error between the constrained idealized image positions and those of the arless data. This irreducible residual is due solely to the constraints imposed by the linkage and indicates the quality with which the linkage reproduces the kinematics of the volunteer.

The purpose of the linkage analysis is to find, for the kinematics of any single volunteer, the geometrical parameters with which the candidate linkage best approximates the arless data. This approximation is that which produces the smallest irreducible residual squared and summed over the entire data set.

This search for the geometrical parameters superimposes a second least squares calculation for the articulational parameters. But, since articulational parameters are calculated for every position in the data set, there are a staggering number of unknowns involved. The crux of the matter is this: The search for the geometrical parameters establishes crosstalks between the formerly independent calculations for the various sets of articulational parameters. Instead of solving n sets of 10 equations in 10 unknowns, the task is now solving n times 10 plus eight (eight geometrical parameters) equations in n times 10 plus eight unknowns.

Fortunately, this new formulation yields readily to a little manipulation. The matrix arithmetic described in appendix A obtains, in a single pass over the data set, the sums

7

necessary to solve for a linearized approximation to the best possible set of the eight geometrical parameters. Although the development indicates that the articulational parameters can be determined by a second pass over the data set, since the search for the geometry is iterative, this second pass is never undertaken.

Although it is possible to solve the eight simultaneous equations in eight unknowns directly to obtain estimates for the geometrical parameters, a more complex approach is taken. The main reason for this more complex approach is that it is extremely likely that the equation set is very nearly singular. That is instead of a single optimum the data can be satisfied equally well by a range of geometrical parameters.

If such a range of solutions is indeed the case, then an iteration using straightforward techniques would at best obtain only a single parameter set from this range and could fail to converge on an optimum at all. Thus, the approach first taken supplied an interactive operator with the results of the eigenvector analysis described in appendix C so that he might select the geometry of successive iterations directly. After this technique had been exercised a number of times, the selection technique was automated and the operator removed from the iteration.

The advantages offered by the eigenvalue analysis is that it transforms the eight simultaneous equations in the eight geometrical parameters into eight independent equations operating each on a different linear combination of these eight parameters. The analysis also shows which of these various linear combinations will most improve the geometry and which, if any, have little or no effect on linkage performance.

The automated technique solves these independent equations and applies the solutions in order of descending importance to obtain the geometry for the next iteration. After the final iteration, the investigator obtains a local optimum linkage and a statement showing how variations of this linkage will affect the total performance.

8

The Application

This linkage analysis was applied to impact data collected on a single human volunteer. This particular volunteer is a healthy, male, naval recruit and has met the stringent physical requirements for participation in the NAMRLD acceleration program. Table 1 lists a number of anthropometric measures and calculations for this volunteer as performed and reported by C. Clauser and K. Kennedy of the 6570th Aerospace Medical Research Laboratory at Wright Patterson Air Force Base. His sitting height, 93.5 cm, is in the 67th percentile of sitting height for the population of naval aviators described in ref. 6.

The impact data was taken from four acceleration experiments, two lateral impacts (G_{+y}) at nominal peak sled accelerations of 6 and 11 G's respectively; and two oblique impacts $(G_{+y - x})$ of 7 and 12 G's. The methodology with which these experiments were conducted is essentially that reported in references 7 and 8. In addition to this impact data, three sets of voluntary motion data were also analyzed. This voluntary motion data is collected in precisely the same manner as the impact data except that instead of undergoing impact, the volunteer moves his head through a rehearsed trajectory. These trajectories include pitch motion in which the volunteer throws his head and neck forward simulating the purely midsagittal responses observed in frontal (G_{-x}) impact; roll motion in which the head and neck are rolled from left to right while continuing to face forward; and yaw motion in which the head is rotated about the z axis as in naying.

The voluntary motion was incorporated into the analysis in lieu of frontal impact data which as yet has not been collected on this particular volunteer. The yaw motion was of particular interest because it was not observed at all in the impact response.

TABLE 1

SUBJECT NUMBER   H-093

Measurement	Value	Measurement	Value
USUAL WEIGHT	164 LBS	WEIGHT AT 18	160 LBS
WEIGHT AT 23	0 LBS	MEASURED WEIGHT	160 LBS
AGE	18 YRS	STATURE	1730 MM
CERVICALE HT	1479 MM	CHIN/NECK HT	1492 MM
SUPRASTERNALE HT	1398 MM	SUBSTERNALE HT	1215 MM
10TH RIB HT	1117 MM	TROCHANTERION HT	886 MM
TIBIALE HT	468 MM	LAT MALLEOLUS HT	73 MM
SUBSCAPULAR SKF	102 MM/10	TRICEPS SKF	66 MM/10
JN SKF	99 MM/10	MALX SKF	95 MM/10
ILIAC CREST	188 MM	MED CALF R	78 MM
CHEST CIRC	977 MM	10TH RIB CIRC	824 MM
BUTTOCK CIRC	960 MM	UPPER THIGH CIRC	595 MM
KNEE CIRC	391 MM	CALF CIRC	370 MM
ANKLE CIRC	237 MM	CALF CIRC L	379 MM
ARM CIRC AXLIRY R	315 MM	BICEPS CIRC FLXD R	323 MM
BICEPS CIRC RLXD R	301 MM	FORARM CIRC RLXD R	270 MM
WRIST CIRC	175 MM	HAND CIRC META III	214 MM
BICEPS CIRC FLXD L	321 MM	RIACROMIAL BREADTH	416 MM
CHEST BREADTH	348 MM	10TH RIB BREADTH	303 MM
WAIST BREADTH	304 MM	BICRISTALE BREADTH	273 MM
HIP BREADTH	348 MM	BISPINOUS BREADTH	209 MM
CHEST DEPTH	226 MM	10TH RIB DEPTH	206 MM
WAIST DEPTH	208 MM	HIP DEPTH	229 MM
ACRNM-RDLF LENGTH	308 MM	BALL OF HUM-RAD	290 MM
RAD STYLION LENGTH	243 MM	FOOT LENGTH	259 MM
HAND LENGTH	193 MM	CERVICALE HT S	684 MM
SHOULDER HT S	614 MM	EYE HT S	817 MM
TRAGION HT S	798 MM	HAND BREADTH META	89 MM
WRIST BREADTH BONE	57 MM	ELBOW BREADTH PT	70 MM
ELBOW BREADTH LEFT	70 MM	SITTING HT	935 MM
T1 TO TOP OF HEAD	266 MM	T1 TO RT TRAGION H	112 MM
FEMUR BREADTH RT	98 MM	FEMUR BREADTH LEFT	96 MM
HEAD CIRC	521 MM	HEAD LENGTH	178 MM
HEAD BREADTH	144 MM	BITRAGION BREADTH	132 MM
TOP HEAD TO TRAG	126 MM	TOP HEAD TO PROSTH	183 MM
WALL TO TRAGION	97 MM	WALL TO PROSTHION	180 MM
A-P DEPTH AT THELT	200 MM	ASIS R-*SYMPH	131 MM
ASIS L-*SYMPH	126 MM		

RESULTS

Although a number of analyses were attempted in which various weighting schemes were applied to the data from the impact and voluntary motion runs, a single finding was common to all of them: The four pivot linkage as described cannot accommodate all of the various head and neck motions encountered in the data. There is a conflict, seemingly, between the voluntary yaw motion and everything else.

However, since this yaw motion is not observed in any of the impact responses, the linkage is still considered a viable candidate. But since the linkage cannot accommodate the entire range of head and neck motion, the linkage optimization has been limited to the kinds of motion observed in the impact studies.

Accordingly, the yaw motion has been dropped because it is not observed at all, and the voluntary roll motion has been dropped because it is available in the volunteer's impact response. The voluntary pitch motion has been retained because it is quite similar to what might be encountered in frontal impact and because there is as yet no frontal impact data for this particular volunteer.

The weighting scheme employed took data evenly distributed throughout each of the impact runs and the voluntary pitch motion run. The calculation was such that oblique impact, lateral impact, and voluntary pitch were each weighted equally in the linkage optimization.

As expected, no single optimum was found. Instead, a range of linkage suit the observations equally well. A single linkage in this range has been mobilized to generate the eigenvector analysis and comparisons with the actual kinematics of the volunteer.

This particular linkage shown in figure 4, was selected largely by its mechanical suitability for use in dummy design. However, since this analysis is purely kinematic and

11

no dynamic work has yet been attempted, this particular linkage should be taken as representative of the performance possible with a four pivot mechanism rather than the last word in such mechanisms.

The performance of this linkage versus each of the impact and voluntary motion experiments is shown in table 2. The voluntary yaw result differs dramatically from the other six experiments. However, since this residual is the root mean square residual taken over the entire experiment, even this dramatic difference is understated.

Figure 5 shows this rms residual at various instants throughout each experiment. But even though this residual is the criterion by which the linkage is evaluated, what these values mean in terms of differences between the head and neck position of the volunteer and the best fit of the linkage is not immediately obvious. Figures 6 through 9 show these differences in terms of magnitudes of translational and angular displacement. This translational magnitude is given in meters and is a familiar mathematical concept. The angular magnitude, given in degrees, derives from the fact that the relative orientation between two 3-dimensional coordinate systems may be expressed as a single rotation about a common fixed axis as discussed in references 9 and 10. As shown in these figures, the yaw motion leads to translational and angular displacements of up to 10 centimeters and 30 degrees.

The results of the eigenvector analysis are summarized in tables 3 and 4. This particular treatment attempts to show how the linkage performance might be affected by varying certain combinations of its geometrical parameters. These combinations are mutually independent so that the changes in linkage performance due to variations along a number of these combinations is just the sum of the changes due to each variation.

Table 4 shows just how large the range of acceptable linkage geometries may be. The Columns labeled " +X' (1%)" and "-X' (1%)" show how the given linkage can be modified

12

Table 2

Linkage Performance Summary

Run	Type	RMS Residual Target Image Displacement
LX 2072	Lateral Impact	.014 millimeters
LX 2182	Lateral Impact	.019
LX 2813	Oblique Impact	.019
LX 2904	Oblique Impact	.012
LX 2967	Voluntary Pitch	.017
LX 2969	Voluntary Roll	.020
LX 2971	Voluntary Yaw	.057
Weighted average	Equal weighting on each of three types	.017 millimeters

13

Table 3

Geometrical Parameters

	T_{1x}	T_{1z}	L_1	L_2	L_3	L_4	H_x	H_z
1	.206	.447	-.283	.416	-.275	.422	-.237	-.442
2	.824	-.497	.164	.079	-.032	.074	.130	-.129
3	.151	.271	-.363	.143	-.201	-.494	.684	-.003
4	-.293	-.012	.734	.342	-.230	-.025	.300	-.338
5	-.250	-.257	-.276	-.282	.273	.454	.476	-.457
6	.288	.582	.329	-.076	.615	.175	.204	.117
7	-.155	-.271	-.194	.770	.480	.008	.025	.199
8	-.029	-.002	.027	.057	-.383	.579	.317	.642

Eigenvectors
(Combinations)

14

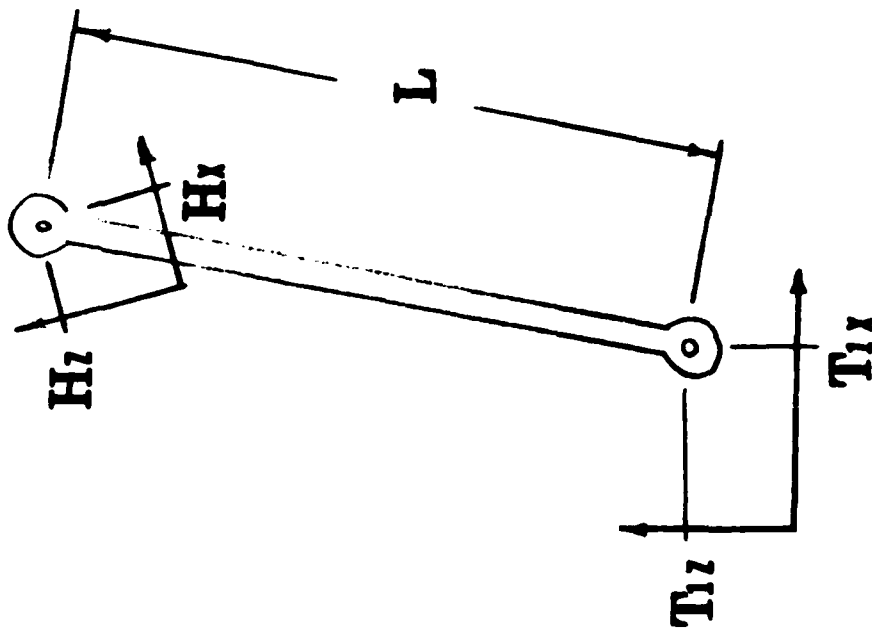# Table 4

Mean Square Residual Versus Linkage Variations

$$E(x') = \sum_{a=1}^{8} \left[D_{aa} (X'_a)^2 - 2 B'_a X'_a \right] + E_o$$

(Equation (6) from appendix C)

$$E_o = .275 \times 10^{-3} \ MM^2$$

	D_{aa} (dimensionless)	B'_a MM	X' Minima MM	+X' (1%) MM	-X' (1%) MM
1	$.474 \times 10^{-5}$	$.347 \times 10^{-5}$	0.7	1.05	0.3
2	$.677 \times 10^{-7}$	$- .302 \times 10^{-7}$	- 0.4	6.0	- 0.8
3	$.509 \times 10^{-7}$	$- .359 \times 10^{-7}$	- 0.7	6.7	- 0.1
4	$.931 \times 10^{-8}$	$- .312 \times 10^{-6}$	- 33.0	4.1	- 7 .
5	$.599 \times 10^{-8}$	$.192 \times 10^{-6}$	32.0	70.5	- 0.5
6	$.863 \times 10^{-9}$	$- .153 \times 10^{-6}$	- 177.	8.8	- 36 .
7	$.200 \times 10^{-9}$	$.525 \times 10^{-8}$	26.	147.	- 94 .
8	$.899 \times 10^{-10}$	$- .442 \times 10^{-7}$	- 492.	30.	- 101 .

FOUR PIVOTS

TWO PIVOTS
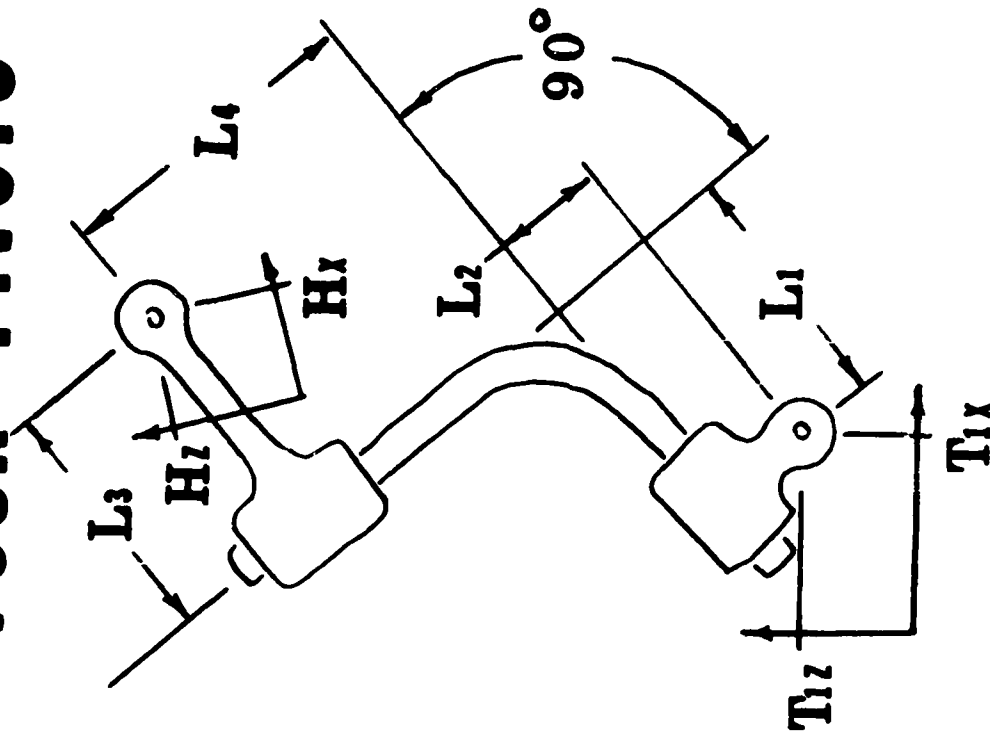
Figure 1. 2D & 3D Linkage Forms

16
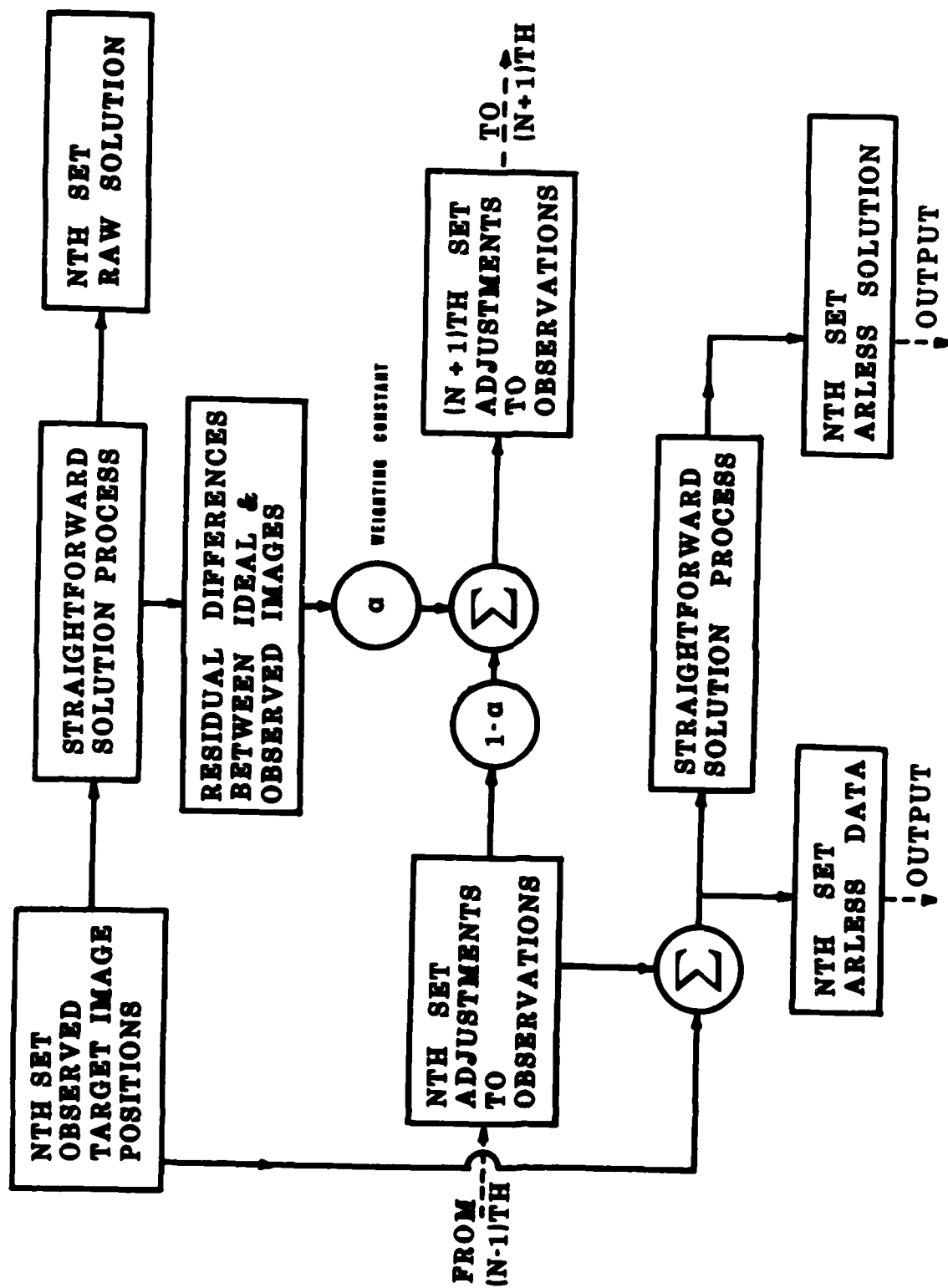
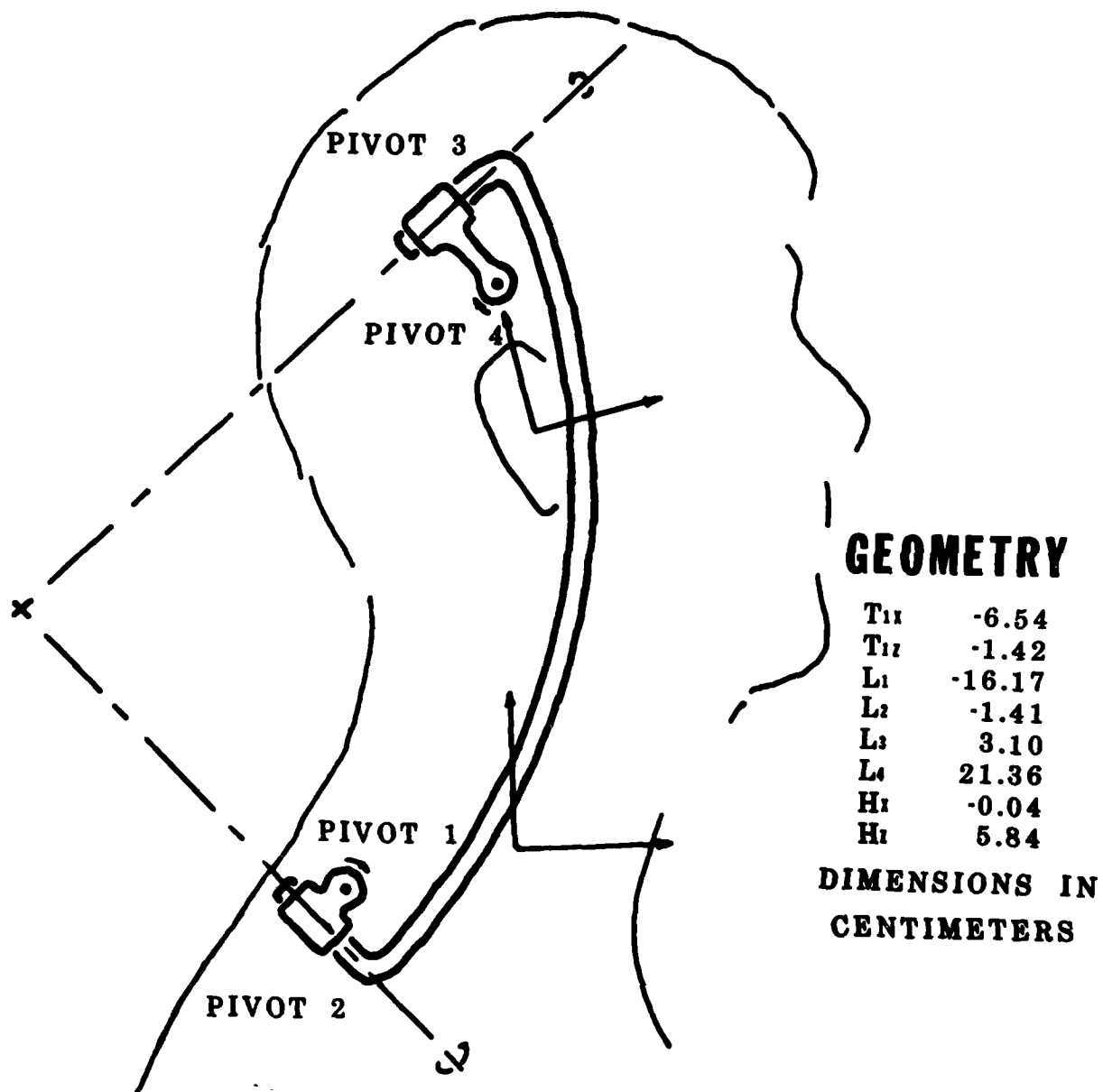Figure 2. An Instrumented Volunteer

Figure 3. The Arless Algorithm

18

GEOMETRY

T_{1x}	-6.54
T_{1z}	-1.42
L_1	-16.17
L_2	-1.41
L_3	3.10
L_4	21.36
H_1	-0.04
H_2	5.84

DIMENSIONS IN
CENTIMETERS

Figure 4. A Suitable Linkage Candidate

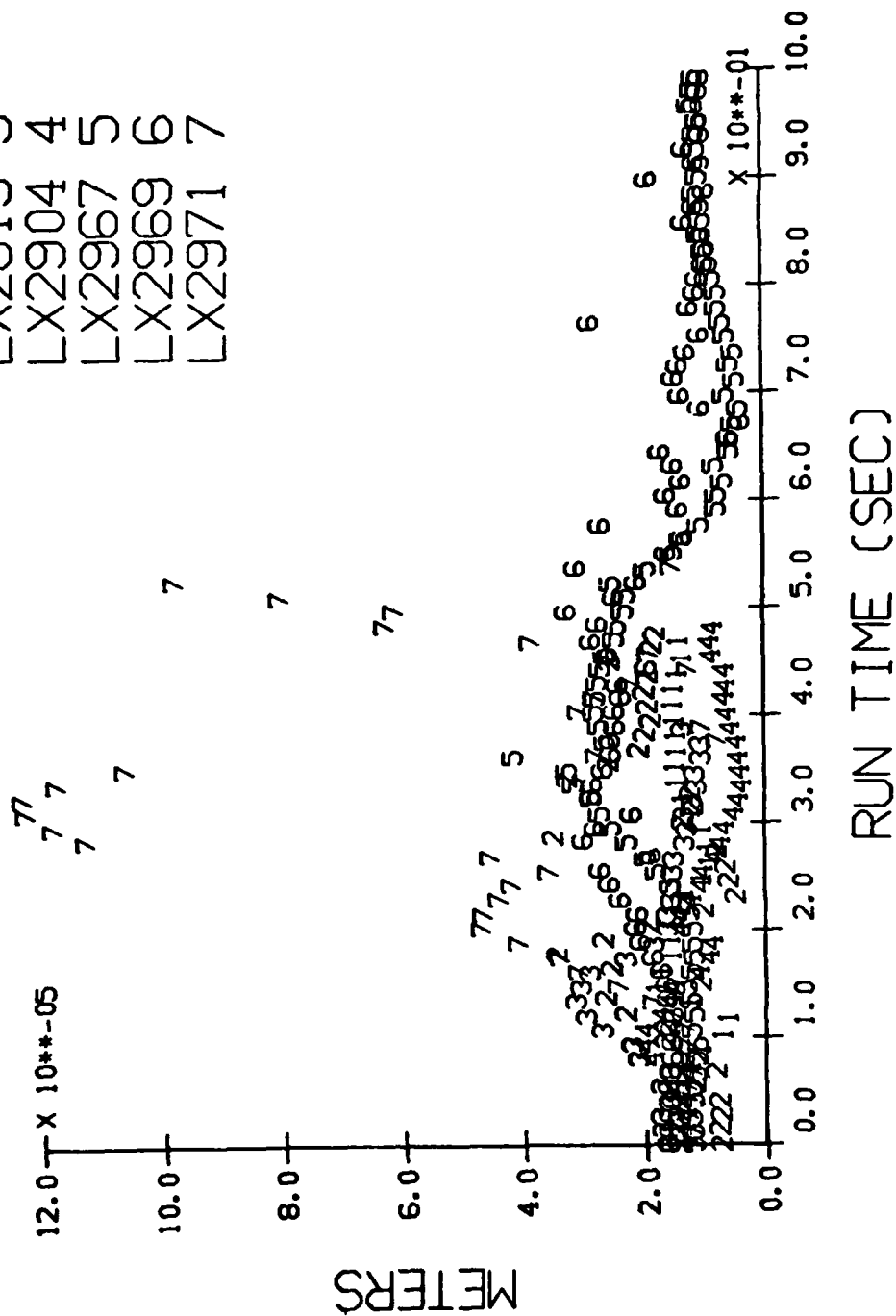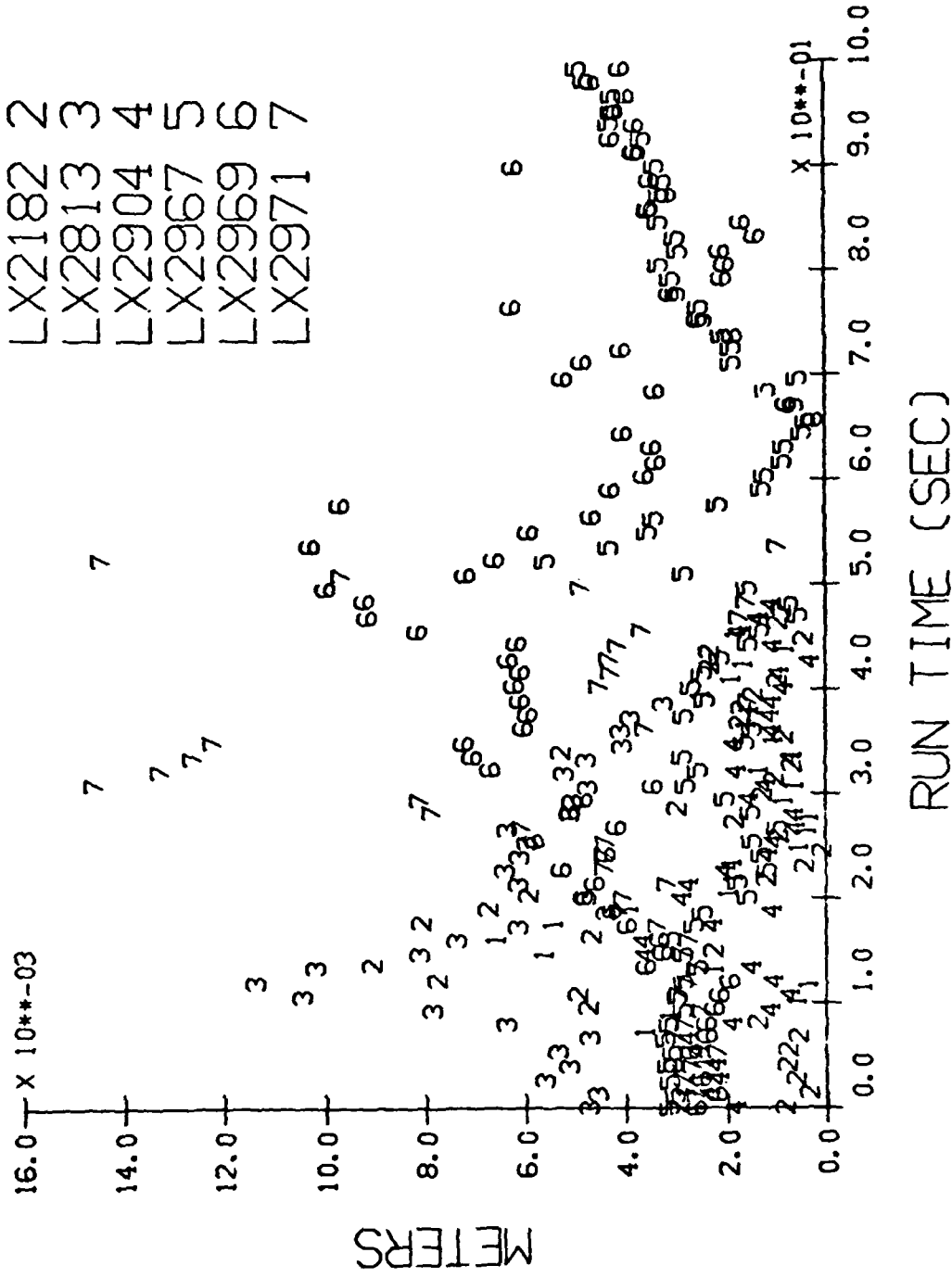Figure 5. Linkage Performance - Residual Error

Figure 6. Linkage Performance - T-1 Displacement

LINKAGE - ARLESS
HEAD DISPLACEMENT
MAGNITUDE

H-093
DATE 02/22/80
LX2072 1
LX2182 2
LX2813 3
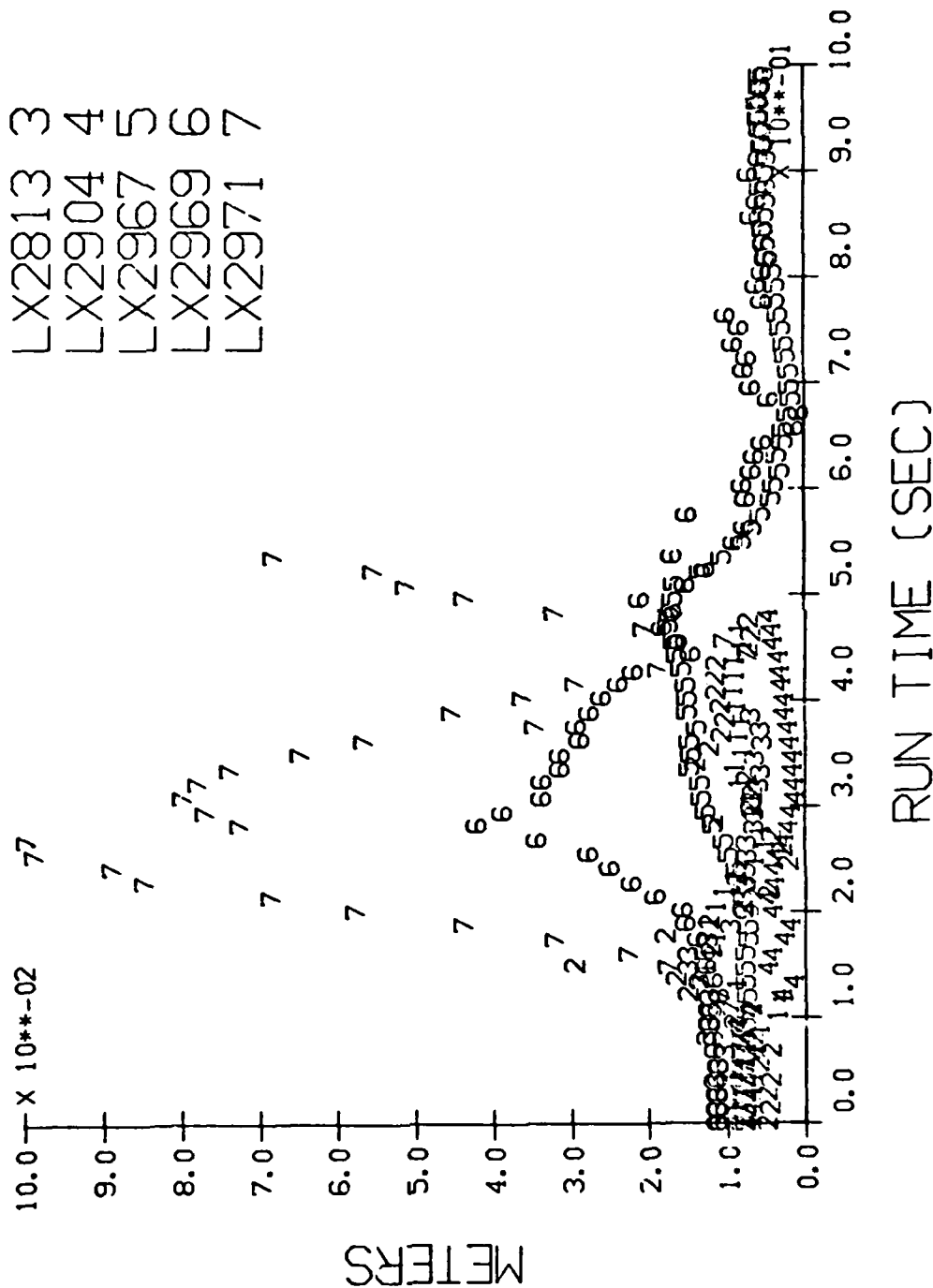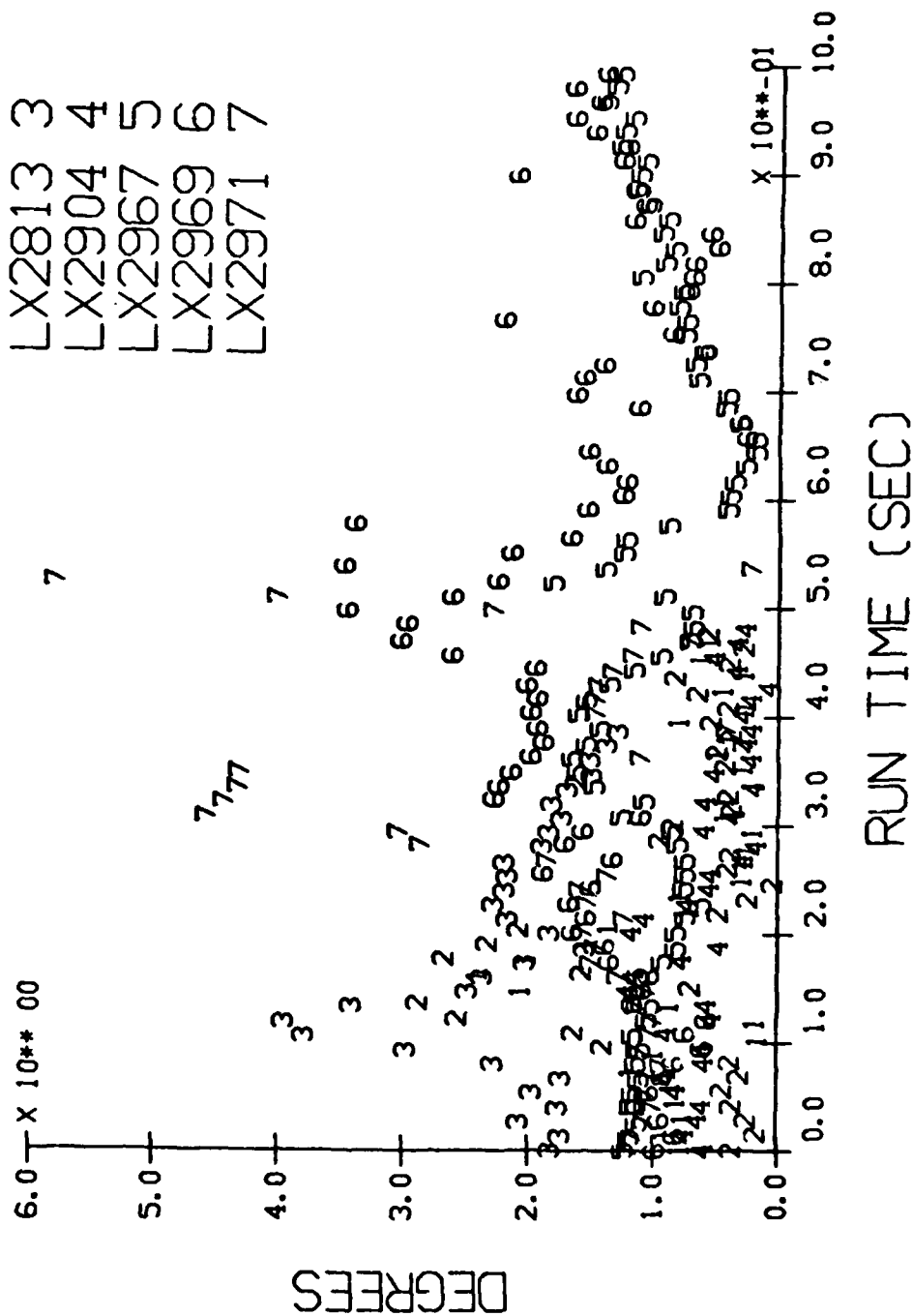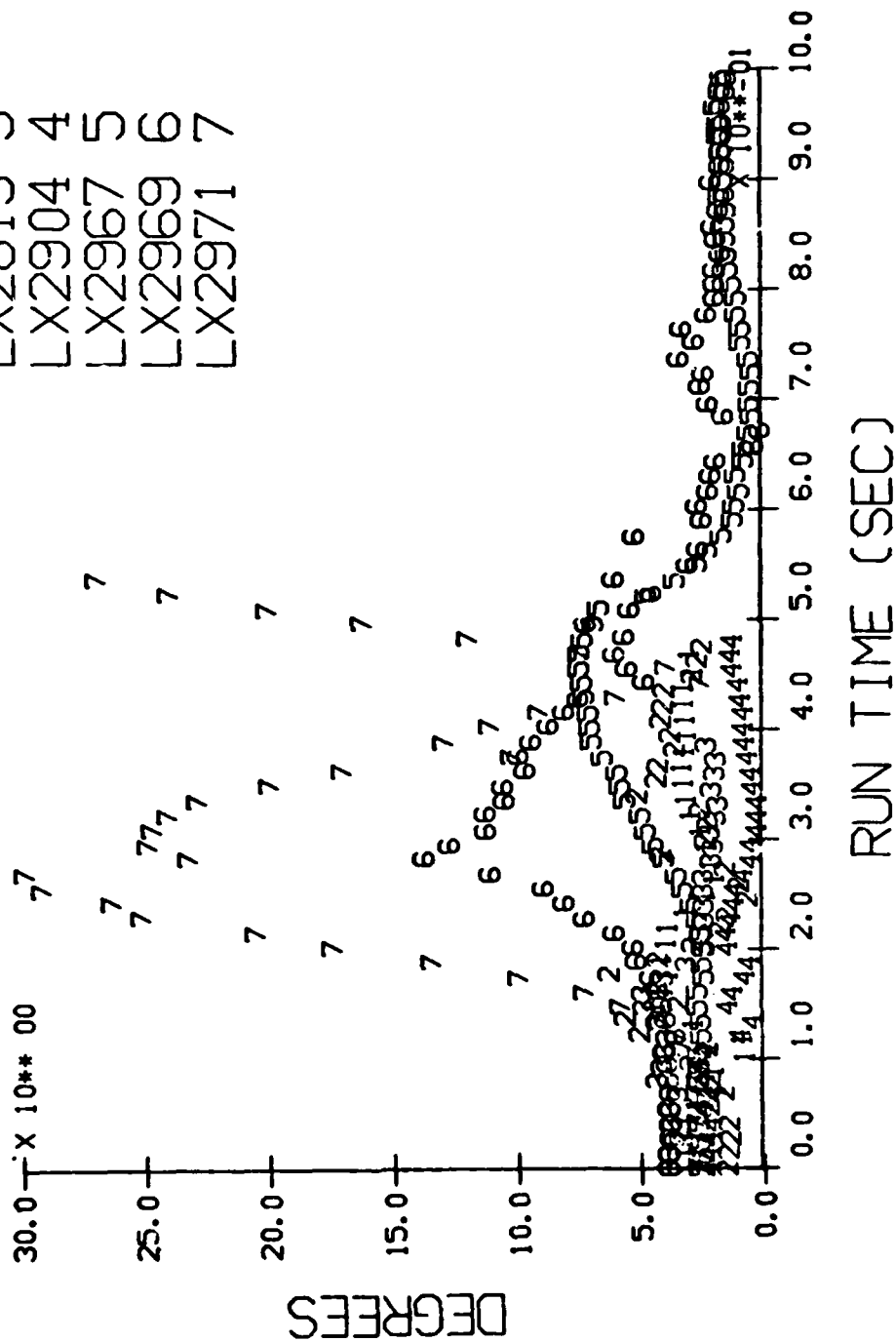LX2904 4
LX2967 5
LX2969 6
LX2971 7

METERS

RUN TIME (SEC)

Figure 7. Linkage Performance - Head Displacement

22

Figure 8. Linkage Performance - T-1 Disorientation

Figure 9. Linkage Performance - Head Disorientation

without increasing the mean square residual beyond one percent of its present value. The first eigenvector, or combination, has a range of about one millimeter; but for the eighth eigenvector this range is well over a meter.

The column labeled "X' Minima" is the theoretical position in terms of these eigenvectors of the absolute optimum linkage. Comparing this column to other two indicates that the given linkage is close to the edge of the given range. In fact, the figures indicate that the total residual could be reduced by as much as 25% for a 13% reduction in the rms residual merely by using this theoretical solution.

Unfortunately, since this eigenvector analysis is based on linear approximations, it should not be extended beyond the near neighbors of the given linkage. By modifying the candidate linkage by five centimeters at a time and reinvoking the eigenvector analysis to reduce the total residual one quickly will arrive at a linkage that is completely unworkable and whose performance is only marginally better than that given.

CONCLUSIONS

The techniques described here are a workable means of fitting a proposed linkage form to photographic data showing human kinematics in response to impact or in voluntary motion.

The particular linkage form selected, a four pivot mechanism, shows promise for use in modeling human head and neck response to frontal, lateral, and oblique impact. Unfortunately, the linkage cannot include voluntary yaw motion in its range of articulation.

This particular inadequacy may well be ignored as such yawing motion has not been observed in the impact experiments performed at this Laboratory.

This work has shown that a range of linkage geometries will serve the observed kinematics equally well. This finding is probably generally true of simple mechanical simulations of the human spine and cervical column

25

The limited angular motions involved as well as the distributed articulation over a large number of joints should serve to make the pivots of simple models indistinct. This is surely the case in the two dimensional model of the human spine identified by Mital, et al in reference 11. In this work calculations based on photographic coverage of the motion of a cadaveric subject's pelvis and T-1 in response to frontal impact led to the geometry of a two pivot linkage. The investigators were then able to alter this geometry considerably to obtain a mechanically feasible linkage that still seemed to serve the observed kinematics.

Since this work is the first part of a two part approach, much of its utility depends on the success of the second part, the dynamic modeling effort. However, it is absolutely crucial that this kinematic modeling be extended to other human volunteers. Until it can be shown that this linkage is generally applicable to the impact kinematics of human beings the work presented here is at best a curiosity.

REFERENCES

1. J. King Foster, James O. Kortge, and Michael J. Wolanin, "Hybrid III - A Biomechanically Based Crash Test Dummy." Paper 770938. Proceedings of Twenty-First Stapp Car Crash Conference, Society of Automotive Engineers, Inc., 400 Commonwealth Drive, Warrendale, PA, 1977.

2. William H. Muzzy III and Leonard Lustick, "Comparison of Kinematic Parameters Between Hybrid II Head and Neck System with Human Volunteers for -Gx Acceleration Profiles." Paper 760801. Proceedings of Twentieth Stapp Car Crash Conference, Society of Automotive Engineers, Inc., 400 Commonwealth Drive, Warrendale, PA, 1976.

3. E. B. Becker, "Preliminary Discussion of An Approach to Modeling Living Human ead and Neck Response to Impact Acceleration." Human Impact Response, Ed. W. F. King and H. J. Mertz, New York: Plenum Press, pp. 321-329, 1973.

4. E. B. Becker, "A Photographic Data System for Determination of 3-Dimensional Effects of Multi Axis Impact Acceleration on Living Humans." Proceedings, Society of Photo-Optical Instrumentation Engineers, Voi. 57. SPIE, Box 1146, Palos Verdes Estates, CA 90274, 1975.

5. E. B. Becker, "Stereoradiographic Measurements for Anatomically Mounted Instruments." Paper 770926. Proceedings of Twenty-First Stapp Car Crash Conference, Society of Automotive Engineers, Inc., 400 Commonwealth Drive, Warrendale, PA, 1977.

6. E. C. Gifford, J. R. Provost, and J. Lazo, "Anthropometry of Naval Aviators - 1964." NAEC-ACEL Report 533, Naval Air Engineering Center, Aerospace Crew Equipment Laboratory, Philadelphia, PA, 1965.

7. C. L. Ewing, D. J. Thomas and L. Lustick, "Multi Axis Dynamic Response of the Human Head and Neck to Impact Acceleration." AGARD Conference Proceedings No. 253, Models and Analogues for the Evaluation of Human Biodynamic Response, Performance and Protection, Paris, France, 1978.

8. C. L. Ewing, D. J. Thomas, L. Lustick, W. H. Muzzy III, G. C. Willems, and P. Majewski, "Dynamic Response of the Human Head and Neck to +Gy Impact Acceleration." Paper 770928. Proceedings of Twenty-First Stapp Car Crash Conference, Society of Automotive Engineers, Inc., 400 Commonwealth Drive, Warrendale, PA, 1977.

9. E. L. Mitchell and A. E. Rogers, "Quaternion Parameters in the Simulation of A Spinning Rigid Body." Simulation, John McLeod (Ed.) McGraw-Hill, 1968.

10. E. B. Becker, "Transforming Anatomically Acquired Kinematic Parameters to Inertially Referenced Coordinates." Fifth Annual International Workshop on Human subjects for Biomechanical Research, Committee Reports and Technical Discussion, New Orleans, LA, 1977.

27

11. Naveen K. Mital, Richard Cheng, Robert S. Levine, and Albert I. King, "Dynamic Characteristics of the Human Spine During -Gx Acceleration." Paper 780889. Proceedings of Twenty-Second Stapp Car Crash Conference, Society of Automotive Engineers, Inc., 400 Commonwealth Drive, Warrendale, PA, 1978.

ACKNOWLEDGEMENTS

SYMBOL TABLE - APPENDIX A

X_{ai} — Ideal value of the ith observation in the ath set of observations

σ_{ak} — Sets of local variables that apply respectively to the sets of observations

Φ_m — A set of global variables that applies to all the observations

O_{ai} — Observed values

X_{oai}

a_{ajk} } Known constants

ba_{im}

AA_a

AB_a } Two dimensional matrices composed of various sums

A_a

BB

δ — The Kronecker delta

BE_a

} Vectors composed of various sums

AE_a

Two Level Optimization

Assume

$$X_{\alpha j} = X_{o\alpha j} + a_{\alpha jk}\,\sigma_{\alpha k} + b_{\alpha jm}\,\Phi_m \qquad \text{no sum on } \alpha \qquad (1)$$

$X_{\alpha j}$ Ideal values of $= 1 \rightarrow \alpha M$ sets

       $J = 1 \rightarrow JM$ observations each

$\Phi_{\alpha k}$ Sets of local variables that apply respectively to these sets of observations

       e.g. the articulation of a linkage

Φ_m Global variables that apply to all the observations, e.g. the geometry

       of that linkage

$X_{o\alpha j}, a_{\alpha jk}, b_{\alpha jm}$ known constants

Find the best fits for $\sigma_{\alpha k}$ and Φ_m given

$O_{\alpha j}$ – observed values of $X_{\alpha j}$

Least Squares Criteria

Find σ_{ak} and Φ_m such that $\sum_a \sum_i (O_{ai} - X_{ai})^2$ is a minimum; that is find σ_{ak}

and Φ_m that satisfy

$$
\begin{bmatrix}
|AA_1| & O & O & \cdots & O & |AB_1|^T \\
O & |AA_2| & O & \cdots & O & |AB_2|^T \\
O & O & |AA_3| & \cdots & O & |AB_3|^T \\
\vdots & \vdots & \vdots & \ddots & \vdots & \vdots \\
O & O & O & \cdots & |AA_{aM}| & |AB_{aM}|^T \\
|AB_1| & |AB_2| & |AB_3| & \cdots & |AB_{aM}| & |BB|
\end{bmatrix}
\begin{bmatrix}
\sigma_{11} \\ \sigma_{kM} \\ \sigma_{21} \\ \sigma_{2kM} \\ \sigma_{31} \\ \vdots \\ \sigma_{aM} \\ \Phi_1 \\ \vdots \\ \Phi_{mM}
\end{bmatrix}
=
\begin{bmatrix}
\sum_i \{ a_{1ik}(O_{1i} - X_{o1i}) \} \\
\sum_i \{ a_{2ik}(O_{2ik} - X_{o2i}) \} \\
\sum_i \{ a_{3ik}(O_{3i} - X_{o3i}) \} \\
\vdots \\
\sum_i \{ a_{aMik}(O_{aMi} - X_{oaMi}) \} \\
\sum_i \sum_a \{ b_{aim}(O_{ai} - X_{oai}) \}
\end{bmatrix}
\quad (2)
$$

$$|AA_a| = \sum_i a_{aik} \, a_{ail}$$

$$|AB_a| = \sum_i a_{aik} \, b_{aim}$$

$$|BB| = \sum_i \sum_a b_{aim} \, b_{ail}$$

This matrix formulation is potentially quite large and also contains many zero elements. Solving for σ_{ak} and Φ_m by straightforward matrix inversion techniques would be at best clumsy and in-ficient. At worst, limitations on computer core and word length would render such a solution meaningless, if not impossible.

Although it is possible to obtain a simpler formulation by direct manipulation of equation (2)
a clearer development might be obtained as follows:

Instead of solving directly for the best fits of $\sigma_{\alpha k}$ and Φ_m, solve for the best fit of
σ_k as a function of Φ_m

$$\sigma_{\alpha k}^{*}(\Phi_m) = \left(\sum_j \left(^a\sigma_{jk}\ ^a\sigma_{jl}\right)\right)^{-1} \left(\sum_j \left\{^a\sigma_{jl}\left(O_{\alpha j} - X_{o\alpha i} - b_{\alpha jm}\Phi_m\right)\right\}\right) \tag{3}$$

where the superscript * indicates a best fit

Now substitute this expression for $\sigma_{\alpha k}^{*}(\Phi_m)$ back into equation (1) and rearrange to get

$$X_{\alpha i} = X_{o\alpha i} + A_{\alpha js}\left(O_{\alpha s} - X_{o\alpha s}\right) + \left(\delta_{js} - A_{\alpha js}\right) b_{\alpha sm}\Phi_m \tag{4}$$

where

$$A_{\alpha js} = \ ^a\sigma_{jk}\ \left(\sum_r\ ^a\sigma_{rk}\ ^a\sigma_{rl}\right)^{-1}\ ^a\sigma_{sl}$$

and

$$\begin{aligned}\delta_{js} &= 1, \quad j = s\\ \delta_{js} &= 0, \quad j \neq s\end{aligned}$$

Now find the best fit for Φ_m

$$\Phi_m = \left[\sum_\alpha \left[\left(\delta_{sj} - A_{\alpha sj}\right)\left(\delta_{st} - A_{\alpha st}\right) b_{\alpha jm} b_{\alpha tn}\right]\right]^{-1} \tag{5}$$

$$\left[\sum_\alpha \left[\left(\delta_{vu} - A_{\alpha vu}\right)\left(\delta_{vw} - A_{\alpha vw}\right) b_{\alpha ur}\left(O_{\alpha w} - X_{o\alpha w}\right)\right]\right]$$

The unique structure of the matrices A_α makes them symmetric and idempotent, that is

$$A_{\alpha js}\ A_{\alpha st} = A_{\alpha jt} = A_{\alpha tj}$$

As a result $\delta - A_\alpha$ is also idempotent so that equation (5) may be rewritten

$$\Phi_m = \left\{ \sum_\alpha \left(b_{\alpha jm} \left(\delta_{jt} - A_{\alpha jt} \right) b_{\alpha tn} \right) \right\}^{-1} \left\{ \sum_\alpha \left(b_{\alpha un} \left(\delta_{uv} - A_{\alpha uv} \right) \left(O_{\alpha v} - X_{o\alpha v} \right) \right) \right\} \qquad (6)$$

Since $\delta - A_\alpha$ can itself be quite large, especially if $_{i}M$ is large; mobilizing equation (6) directly may also prove quite cumbersome. However, this equation may be rewritten to eliminate $\delta - A_\alpha$ yielding

$$\delta_m^{\cdot} = \left\{ \sum_\alpha \left(BB_{\alpha mn} - BA_{\alpha mk} \, AA_{\alpha kl}^{-1} \, BA_{\alpha nl} \right) \right\}^{-1}$$

$$\left\{ \sum_\alpha \left(BE_{\alpha n} - BA_{\alpha nk} \, AA_{\alpha kl}^{-1} \, AE_{\alpha l} \right) \right\}$$

Where

$$BB_{\alpha mn} = \sum_i b_{\alpha jm} \, b_{\alpha jn}$$

$$BA_{\alpha mk} = \sum_i b_{\alpha jm} \, a_{\alpha jk}$$

$$AA_{\alpha kl} = \sum_i a_{\alpha jk} \, a_{\alpha jl}$$

$$BE_{\alpha n} = \sum_i \left[b_{\alpha jn} \left(O_{\alpha j} - X_{o\alpha j} \right) \right]$$

$$AE_{\alpha l} = \sum_i \left[a_{\alpha jl} \left(O_{\alpha j} - X_{o\alpha j} \right) \right]$$

Note: In general, repetition of indices implies summation except that index represented by α

A-4

SYMBOL TABLE - APPENDIX B

X   Vector in three dimensional coordinates

Φ Transformation matrix or pivot rotation

C   Transformation matrix

Superscript primes denote successive coordinate systems

Superscript T denotes matrix transpose

Subscript a denotes pivot location

Subscript 1,2,3 identifies pivot

The Linkage Candidate

The constraint that a pivot puts on the relative positions of two coordinate systems may be written

$$\underline{X} = \underline{\emptyset}_a \ (\underline{X}' - \underline{X}'_a) + \underline{X}_{-a} \tag{1}$$

where $\underline{\emptyset}_a$ can be described as

$$\underline{O}_a = \underline{C}^t \begin{vmatrix} \cos \emptyset & 0 & \sin \emptyset \\ 0 & 1 & 0 \\ -\sin \emptyset & 0 & \cos \emptyset \end{vmatrix} \qquad \underline{C} = \underline{C}^t \ \underline{O}_y \ \underline{C}' \tag{2}$$

That is rotation about a single axis oriented by $\underline{C}$ in the $\underline{X}$ system and by $\underline{C}'$ in the $\underline{X}'$ system. $\underline{X}_a$ and $\underline{X}'_a$ represent a single point on this axis in $\underline{X}$ and $\underline{X}'$ respectively.

A chain of coordinate systems constrained by a sequence of pivots may be described for two pivots as

$$\underline{X} = \underline{\emptyset}_{a1} \ (\emptyset_{a2} \ (\underline{X}'' - \underline{X}''_{a2}) + \underline{X}'_{-a2} - \underline{X}'_{-a1}) + \underline{X}_{-a1} \tag{3}$$

and for many pivots as

$$\underline{X} = \underline{\emptyset}_{a1} \ (\underline{\emptyset}_{a2} \ (\ldots \underline{\emptyset}_{an} (\underline{X}^n - \underline{X}^n_{an}) + \underline{X}^{n-1}_{-an} \ \ldots) + \underline{X}'_{a2} - \underline{X}'_{a1}) + \underline{X}_{-a1} \tag{4}$$

Since the interior coordinate systems of these linkages are of little interest, they may be oriented and located as necessary to simplify these expressions. Rewriting equation (3) yields

$$\underline{X} = \underline{C}^t_1 \ \underline{\emptyset}_{y1} \ \underline{C}'_1 \ \underline{C}'^t_2 \ \underline{\emptyset}_{y2} \ \underline{C}''_2 \ (\underline{X}'' - \underline{X}''_{a2})$$

$$\tag{5}$$

$$+ \ \underline{C}^t_1 \ \underline{\emptyset}_{y1} \ \underline{C}'_1 \ (\underline{X}'_{-a2} - \underline{X}'_{-a1}) + \underline{X}_{-a1}$$

$\underline{C}'_1 \ \underline{C}'^t_2$ is a coordinate rotation and may be described as successive rotations about $\hat{y}$, carried $\hat{z}$, and carried $\hat{y}$ yielding

$$\underline{C}'_1 \underline{C}'_2 = \underline{C}'_{y1} \underline{C}'_z \underline{C}'_{y2} \tag{6}$$

Furthermore, the vector $(\underline{X}'_{a2} - \underline{X}'_{a1})$ may be similarly broken down to components parallel to $\widehat{y}_1$, $\widehat{z}$, and $\widehat{y}_2$. Since the $\widehat{y}_1$ component is unaffected by rotations about $\widehat{y}_1$ it may be passed backward through $\underline{C}_{y1}$ and $\underline{\emptyset}_{y1}$. The $\widehat{y}_2$ component may be passed forward through $\underline{C}'_{y2}$ and $\underline{\emptyset}_{y2}$ in a similar manner.

If we now select the $\underline{X}'$ system so that $\widehat{z}'$ is perpendicular to the two pivot axes contained in this system then $\underline{C}'_{y1}$ and $\underline{C}'_{y2}$ may be reduced to identify matrixes and the remaining component of $(\underline{X}'_{a2} - \underline{X}'_{a1})$ lies along the z' axis. Equation (5) becomes

$$\underline{X} = \underline{C}^t_1 \underline{\emptyset}_{y1} \underline{C}'_2 \underline{\emptyset}_{y2} \underline{C}''_2 (\underline{X}'' - \underline{X}''_{a2})$$

$$+ \underline{C}^t_1 \begin{vmatrix} 0 \\ y'_1 \\ 0 \end{vmatrix} + \underline{C}^t_1 \underline{\emptyset}_{y1} \begin{vmatrix} 0 \\ 0 \\ z' \end{vmatrix} \tag{7}$$

$$+ \underline{C}^t_1 \underline{\emptyset}_{y1} \underline{C}'_2 \underline{\emptyset}_{y2} \underline{C}''_2 (\underline{C}''^t_2 \begin{vmatrix} 0 \\ y'_2 \\ 0 \end{vmatrix}) + \underline{X}_{a1}$$

Since $\underline{C}^t_1 \begin{vmatrix} 0 \\ y'_1 \\ 0 \end{vmatrix}$ and $\underline{C}''_2 \begin{vmatrix} 0 \\ y'_2 \\ 0 \end{vmatrix}$ are constant

vectors in the $\underline{X}$ and $\underline{X}''$ systems respectively they may be incorporated into $\underline{X}_{a1}$ and $\underline{X}''_{a2}$ respectively to yield

$$\underline{X} = \underline{C}^t_1 \underline{\emptyset}_{y1} \underline{C}'_z \underline{\emptyset}_{y2} \underline{C}''_2 (\underline{X}'' - \underline{X}''_{a2}) \tag{8}$$

$$+ \underline{C}^t_1 \underline{\emptyset}_{y1} \begin{vmatrix} 0 \\ 0 \\ z' \end{vmatrix} + \underline{X}_{a1}$$

B-3

If bilateral symmetry and pivot axes parallel to $\hat{y}, \hat{y}''$, and each other are imposed then the still general expression (8) becomes

$$X = \underset{=y1}{\emptyset}(\underset{=y2}{\emptyset}(\underline{X}'' - \begin{vmatrix} X''_{a2} \\ 0 \\ Z_{a2} \end{vmatrix}) + \begin{vmatrix} 0 \\ 0 \\ Z' \end{vmatrix}) + \begin{vmatrix} X_{a1} \\ 0 \\ X_a \end{vmatrix}$$

This statement has five parameters: X_{a1}, Z_{a1}, Z', X''_{a2}, and Z''_{a2} which correspond to T_{1x}, T_{1z}, L, H_x, and H_z in figure 1.

The four pivot expression resulting from equation (4) is

$$\underline{X} = \underset{=ai}{\emptyset}(\underset{=a2}{\emptyset}(\underset{=a3}{\emptyset}(\underset{=a4}{\emptyset}(\underline{X}'''' - \underline{X}''''_{a4}) + \underline{X}'''_{a4} - \underline{X}'''_{a3})$$

$$+ \underline{X}''_{a3} - \underline{X}''_{a2}) + \underline{X}'_{a2} - \underline{X}'_{a1}) + \underline{X}_{a1}$$

The interior systems and X_a's may be redefined to obtain

$$X = C_1^t \emptyset_{y1} (C_z' \emptyset_{y2} (C''_z \emptyset_{y3} C'''_z (\emptyset_{y4}(X'''' - X''''_{a4}) + \begin{vmatrix} X''' \\ 0 \\ Z''' \end{vmatrix})$$

$$+ \begin{vmatrix} 0 \\ 0 \\ Z'' \end{vmatrix}) + \begin{vmatrix} X' \\ 0 \\ Z' \end{vmatrix}) + \underline{X}_{a1}$$

This derivation began between the two interior pivot axes and proceeded outward to the ends of the linkage. Since components were passed outward only, two of the interior vectors analogous to 0, 0, Z' in equation (7) must also have x components.

This expression may be simplified further by imposing the following requirements: Bilateral symmetry, the first axis is parallel to $\hat{y}$, the second is perpendicular to $\hat{y}$, the third axis is perpendicular to $\hat{y}''''$ and the fourth is parallel to $\hat{y}''''$. It is also assumed

that for the case of zero rotation about the second and third axes that $\hat{y}$ is parallel to $\hat{y}''''$. The expression now becomes

$$\underline{X} = \underline{\emptyset}_{y1} \ (\underline{C}_1 \ \underline{\emptyset}_{y2} \ \underline{C}''_z \ \underline{\emptyset}_{y3} \ \underline{C}^\dagger_\perp \ (\underline{\emptyset}_{y4} \ (\underline{X}'''' - \begin{vmatrix} X''''_{a4} \\ 0 \\ Z''''_{a4} \end{vmatrix} \ )$$

$$+ \begin{vmatrix} X''' \\ 0 \\ Z'' \end{vmatrix} \ ) \begin{vmatrix} X' \\ 0 \\ Z' \end{vmatrix} \ ) + \begin{vmatrix} X_{a1} \\ 0 \\ Z_{a1} \end{vmatrix}$$

The quantity Z'' is an interesting casualty. The requirements on the axis orientations and bilateral symmetry combine to force it to zero.

The rotation $\underline{C}_\perp$ satisfies the perpendicularity requirement. It may be dropped from the expression by altering the forms of the interior rotations to rotations about $\hat{x}$ and $\hat{z}$ axes

$$\underline{X} = \underline{\emptyset}_{y1} \ (\underline{\emptyset}_{x2} \ \underline{C}_y \ \underline{\emptyset}_{z3} \ (\underline{\emptyset}_{y4} \ (X'''' - \begin{vmatrix} X''''_{a4} \\ 0 \\ Z''''_{a4} \end{vmatrix}$$

$$+ \begin{vmatrix} X''' \\ 0 \\ Z''' \end{vmatrix} \ ) + \begin{vmatrix} X' \\ 0 \\ Z' \end{vmatrix} \ ) + \begin{vmatrix} X_{a1} \\ 0 \\ Z_{a1} \end{vmatrix}$$

in this work $\underline{C}_y$ is further assumed to be an identity matrix reducing the description of this system to eight fixed parameters. These are X_{a1}, Z_{a1}, X', Z', X''', Z''', X''''_{a4}, and Z''''_{a4} which correspond to T_{1x}, T_{1z}, L_1, L_2, L_3, L_4, H_x, and H_z in figure 1.

SYMBOL TABLE - APPENDIX C

A   Symmetric matrix

B   Vector

E   Scalor - Mean Square Error

X   Vector - Variation in linkage geometry

C   Orthogonal transformation

D   Diagonalized matrix

APPENDIX C

Eigenvalue Analysis

The essence of the linkage analysis is that it seeks to obtain that linkage geometry for which a single sum is a minimum. This sum is the total of the squared residual differences between the arless data and the best fit to this data by the articulational parameters.

As can be seen, there are two best fit procedures going on simultaneously; one involving the geometrical parameters and the other the articulational parameters. These become the global and local variables respectively of appendix A.

The analysis depends on obtaining linearized approximations of the functional relationships of these residual differences with the various parameters. These linearized relationships can then be used to infer the behavior of that single sum of squared residuals for a range of geometries.

Of course the inference here depends on the reliability of the linearized approximations of the residuals versus the parameters, and these are reliable only in the vicinity of the parameters for which the approximations were derived.

Fortunately, the situation is not quite circular, the approximations may be derived for some parameter set chosen largely by intuition. Then the linea inference can be trusted to identify a better parameter set that is still in the vicinity of the initial guess. Successive iterations of this process may then lead to an optimum linkage for which the sum of the squared residuals is truly a minimum.

The inference is in the form of a single matrix equation called a quadratic form.

$$A_{1j} X_1 X_j - 2 B_1 X_i + E_o = E(X) \tag{1}$$

Where

x represents the difference between any geometry and the set of parameters currently considered:

A is an eight by eight symmetrical matrix and B an eight vector all of whose components are calculated in the various sums of appendix A; E_o is the squared and summed residuals for the particular parameters being considered; and E(X) is the projected value for that sum at a geometry removed by X from the current parameters.

The value of X for which E(X) is a minimum can be derived by applying a little differential calculus

$$\frac{\partial E}{\partial X_i} = 2 A_{ij} X_j - 2 B_i \tag{2}$$

or

$$A_{ij} X_j = B_i \tag{3}$$

The direct solution would then be:

$$X_i = A_{ij}^{-1} B_i \tag{4}$$

which presumably would be added to the current set of geometry to repeat the analysis around this projected minima.

If the projected value of X is large, it is quite possible that the actual value of E will be larger than the projected value and in fact even larger than E_o itself. It is very likely in such a case, that repeated calculation would diverge from the best geometry. Furthermore, if the equations are nearly singular, that is if the matrix A is ill conditioned, X will almost certainly be large.

These difficulties can be circumvented by applying an eigenvector analysis. This technique conjures up an eight dimensional countour map in which each of the eight dimensions corresponds to one of the geometrical parameters and the contours correspond to the values of E(X). These contours are concentric ellipsoids whose corresponding values

of E(X) diminish toward the center.

The eigenvector analysis yields the shape of these ellipsoids and their orientation in space by diagonalizing the matrix $\underline{A}$.

$$A_{ij} = C_{ki} D_{kl} C_{lj}$$

where $\qquad D_{kl} = 0 \quad k \neq l$ \hfill (5)

and $\qquad \underline{C}$ represents an affine transformation.

The matrix $\underline{C}$ represents a transformation to a new set of coordinates in the eight dimensional space. The axes of this new system are parallel to the axes of the concentric ellipsoids. The off-diagonal elements of $\underline{D}$ are equal to zero, but the diagonal elements are inversely proportional to square of the corresponding semi axes of the ellipsoids.

Applying this transformation to equation (1) yields

$$\sum_{a=1}^{8} \left[D_{a a} (X_a')^2 - 2 B_a' X_a' \right] + E_o = E(X') \hfill (6)$$

Where the prime indicates that the vectors have been rotated to the new coordinates. This new equation reduces the contribution of changes in linkage geometry to the total residual error to eight independent contributions.

The advantage of this new formulation is that these eight independent contributions may not be equally important. A small variation along one of these primed axes may produce a large change in E while even large variations along other axes may have only the most negligible effect.

The $\underline{X}'$ for which $E(X')$ is a minimum is

$$X_a' = B_a'/D_{a a} \quad \text{no sum on } a \hfill (7)$$

The corresponding decrease in E for each component of X' is

$$- E_a = (B_a')^2/D_{a a} \quad \text{no sum on} \hfill (8)$$

C-4

and the second derivative of $E(X^1)$ is

$$\frac{\partial^2 E}{\partial X'_a \partial X'_\beta} = \begin{matrix} 2D_{aa} & \beta = a \\ 0 & \beta \neq a \end{matrix} \tag{9}$$

The eigenvector analysis reduces the eight dimensional search to eight independent one dimensional searches. The results of these eight searches may be invoked selectively at the whim of the investigator within the range of the linear approximation.

Furthermore, since D_{aa} is directly proportional to the second derivatives of the eight solutions, it serves to rank them in order of importance. The solution is best defined along the axes for which D_{aa} is greatest. As D_{aa} approaches zero, displacement along the corresponding axis becomes less significant indicating that a range of geometries may serve equally well. Although negative values of D_{aa} are theoretically impossible, round off errors and the like may result in infinitesimal D_{aa}'s being calculated as slightly less than zero. Such D_{aa} may be ignored.

At the outset of the linkage study the results of the eigenvector analysis were displayed to the investigator so that he might select the next candidate geometry directly. On the basis of this experience the routines were restructured to invoke the eight eigenvector solutions in order of descending D_{aa} until a maximum displacement was reached or a maximum decrease in expected E was exceeded. This scheme worked well in practice.

C-5